Food Chemistry 168 (2015) 332–340

Contents lists available at ScienceDirect

Food Chemistry

journal homepage: www.elsevier.com/locate/foodchem

Interaction of chlorogenic acids and quinides from coffee with human serum albumin

Valentina Sinisi [a,*], Cristina Forzato [a], Nicola Cefarin [a], Luciano Navarini [b], Federico Berti [a,*]

[a] Dipartimento di Scienze Chimiche e Farmaceutiche, Università degli Studi di Trieste, via L. Giorgieri 1, 34127 Trieste, Italy
[b] illycaffè S.p.A., via Flavia 110, 34147 Trieste, Italy

ARTICLE INFO

Article history:
Received 10 February 2014
Received in revised form 11 June 2014
Accepted 15 July 2014
Available online 24 July 2014

Keywords:
Human serum albumin
Protein–ligand interaction
Fluorescence spectroscopy
Coffee polyphenols
Chlorogenic acids

ABSTRACT

Chlorogenic acids and their derivatives are abundant in coffee and their composition changes between coffee species. Human serum albumin (HSA) interacts with this family of compounds with high affinity. We have studied by fluorescence spectroscopy the specific binding of HSA with eight compounds that belong to the coffee polyphenols family, four acids (caffeic acid, ferulic acid, 5-*O*-caffeoyl quinic acid, and 3,4-dimethoxycinnamic acid) and four lactones (3,4-*O*-dicaffeoyl-1,5-γ-quinide, 3-*O*-[3,4-(dimethoxy)cinnamoyl]-1,5-γ-quinide, 3,4-*O*-bis[3,4-(dimethoxy)cinnamoyl]-1,5-γ-quinide, and 1,3,4-*O*-tris[3,4-(dimethoxy)cinnamoyl]-1,5-γ-quinide), finding dissociation constants of the albumin–chlorogenic acids and albumin–quinides complexes in the micromolar range, between 2 and 30 μM. Such values are comparable with those of the most powerful binders of albumin, and more favourable than the values obtained for the majority of drugs. Interestingly in the case of 3,4-*O*-dicaffeoyl-1,5-γ-quinide, we have observed the entrance of two ligand molecules in the same binding site, leading up to a first dissociation constant even in the hundred nanomolar range, which is to our knowledge the highest affinity ever observed for HSA and its ligands. The displacement of warfarin, a reference drug binding to HSA, by the quinide has also been demonstrated.

1. Introduction

Phenolic acids are found as secondary metabolites in leaves, roots and especially fruits of many plants. Chlorogenic acids (CGAs) derive from the esterification with D-(−)-quinic acid **1** of certain cinnamic acids, such as caffeic acid **2**, ferulic acid **3** and *p*-coumaric acid **4** (Fig. 1), constituting a large family of different molecules in the form of mono- or multi-esters (Clifford, 2000).

Of all the CGAs present in green coffee beans, which are the best source of CGAs found in plants with an amount of 5–12 g/100 g (Farah, Monteiro, Donangelo, & Lafay, 2008), caffeoylquinic acids (CQAs) represent the main subgroup and 5-*O*-caffeoylquinic acid **5** (5-CQA, Fig. 1) is the most abundant one, indeed it is usually called *chlorogenic acid*. A difference between the two types of coffee was also evidenced since Robusta green coffee turned out to be richer in CGAs than Arabica (Farah, de Paulis, Trugo, & Martin, 2005). The roasting process causes a partial loss of CGAs, due to the occurrence of many reactions including isomerization, degradation, dehydration and lactonization (Fig. 1) (Clifford, 1985; Scholz & Maier, 1990; Schrader, Kiehne, Engelhardt, & Maier, 1996). The latter reaction leads to chlorogenic acid lactones (CGLs) which have also shown potential biological activities (de Paulis et al., 2002).

CGAs and CGLs are extracted during coffee brewing, and their content in the cup depend on the type of roasted coffee used and on the extraction method (Gloess et al., 2013); in a traditional *espresso* coffee beverage (30 ml) the content of monocaffeoyl quinic acids is on average 70 mg (Navarini et al., 2008). The extraction efficiency is higher for CGAs than for CGLs, due to their better water solubility, and in general a *lungo* (about 120 ml) is more rich in CGAs than a regular *espresso* coffee.

Many studies reported that polyphenols are capable to permeate the gastrointestinal barrier and are absorbed in humans, being found in plasma as both intact molecules and as their hydrolysis metabolites, in particular as caffeic acid (Farah et al., 2008; Monteiro, Farah, Perrone, Trugo, & Donangelo, 2007; Nardini, Cirillo, Natella, & Scaccini, 2002; Olthof, Hollman, & Katan, 2001; Renouf et al., 2010); CQAs have been detected in plasma even 4 h after the ingestion.

Abbreviations: CGAs, chlorogenic acids; CQAs, caffeoylquinic acids; 5-CQA, 5-*O*-caffeoylquinic acid; CQLs, chlorogenic acid lactones; DMSO, dimethyl sulfoxide; HSA, human serum albumin; Trp, tryptophan.

* Corresponding authors. Tel.: +39 040 5583920; fax: +39 0405583903.
E-mail addresses: valentina.sinisi@phd.units.it (V. Sinisi), fberti@units.it (F. Berti).

http://dx.doi.org/10.1016/j.foodchem.2014.07.080
0308-8146/

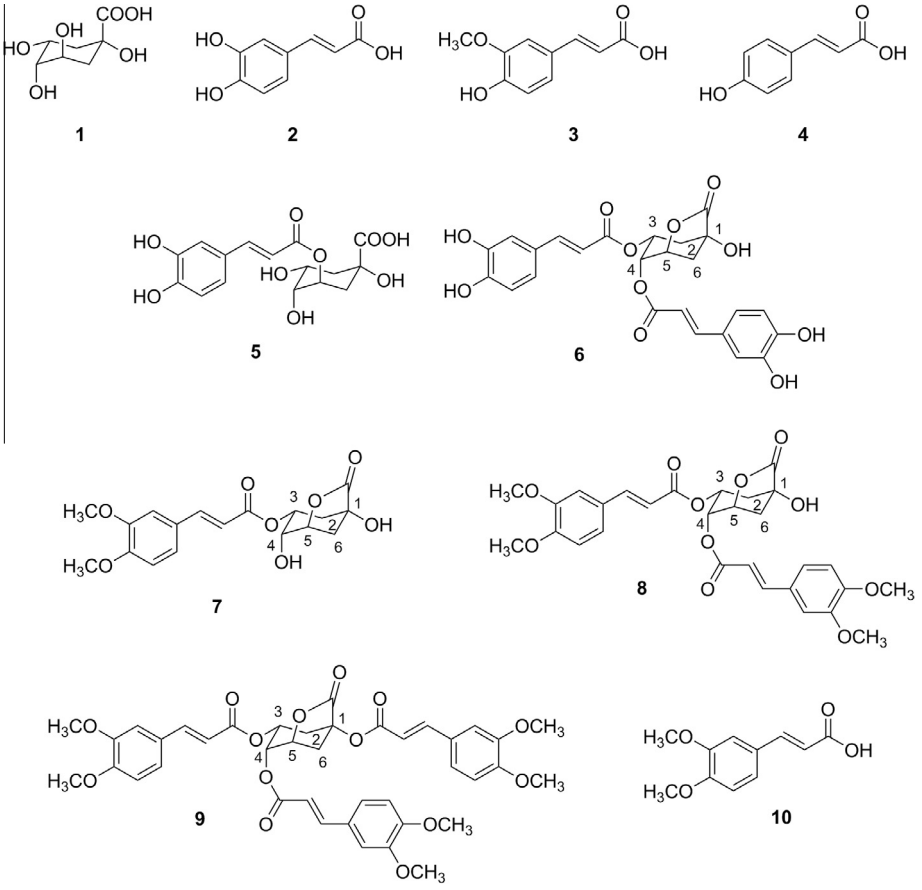

Fig. 1. Molecular structure of (−)-quinic acid (**1**), caffeic acid (**2**), ferulic acid (**3**), *p*-coumaric acid (**4**), 5-*O*-caffeoylquinic acid (**5**) (the IUPAC numbering system for chlorogenic acid (IUPAC, 1976) is adopted and, to avoid confusion, the same numbering system of the carbon atoms both for lactones and for the acid precursors is used), 3,4-*O*-dicaffeoyl-1,5-γ-quinide (**6**), 3-*O*-[3,4-(dimethoxy)cinnamoyl]-1,5-γ-quinide (**7**), 3,4-*O*-bis[3,4-(dimethoxy)cinnamoyl]-1,5-γ-quinide (**8**), 1,3,4-*O*-tris[3,4-(dimethoxy)cinnamoyl]-1,5-γ-quinide (**9**) and 3,4-dimethoxycinnamic acid (**10**).

Human serum albumin (HSA) is the most abundant protein in human plasma, a monomeric 585-residue protein containing three homologous helical domains (I–III), each divided into two subdomains (A and B) (He & Carter, 1992). Two main binding sites for small organic molecules are found, one located in subdomain IIA and one in IIIA, that are known as Sudlow I and Sudlow II sites, respectively (Sudlow, Birkett, & Wade, 1975a).

The protein is able to bind a large variety of endogenous ligands, as non-esterified fatty acids, bilirubin, heme, thyroxine, bile acids; many drugs with acidic or electronegative moieties (including phenols as paracetamol) also exploit the interaction with HSA to be carried in human body (Ghuman et al., 2005; Varshney et al., 2010). Recently an interactive association of multiple ligands with the same binding site inside subdomain II of HSA has been proposed (Yang et al., 2012). As to the binding of phenolic compounds from dietary sources, flavonoids as flavanol, flavonol, flavone, isoflavone, flavanones, and anthocyanidins are known to interact with HSA (Pal & Saha, 2014). The interactions of catechins [(−)-epigallocatechin-3-gallate, (−)-epigallocatechin, (−)-epicatechin-3-gallate], flavones (kaempferol, kaempferol-3-glucoside, quercetin, naringenin) and hydroxycinnamic acids (rosmarinic acid, caffeic acid, p-coumaric acid) with bovine albumin has been reported in this journal by Skrt, Benedik, Podlipnik, and Ulrih (2012). Resveratrol binds to HSA and its interaction is modulated by stearic acid (Pantusa, Sportelli, & Bartucci, 2012). Specific binding of caffeic, ferulic, and 5-CQA acids inside Sudlow site I of HSA has been studied, revealing K_D about 6 μM, 40 μM and 25 μM respectively (Kang et al., 2004; Min et al., 2004; Hu, Chen, Zhou, Bai, & Ou-Yang, 2012). In this study the aim was to extend the knowledge regarding the interaction between polyphenols present in coffee and HSA. For this purpose we have synthesised four quinides of caffeic acid and of 3,4-*O*-dimethoxycinnamoyl acid: 3,4-*O*-dicaffeoyl-1,5-γ-quinide **6**, 3-*O*-[3,4-(dimethoxy)cinnamoyl]-1,5-γ-quinide **7**, 3,4-*O*-bis[3,4-(dimethoxy)cinnamoyl]-1,5-γ-quinide **8**, and 1,3,4-*O*-tris[3,4-(dimethoxy)cinnamoyl]-1,5-γ-quinide **9** (Fig. 1).

Compound **6** is very abundant in roasted coffee, while the class of dimethoxycinnamoylquinic acids, precursors of compounds **7**, **8**, and **9**, was recently found and characterised in green coffee beans (Clifford, Knight, Surucu, & Kuhnert, 2006).

We have measured the dissociation constants to Sudlow site I of our compounds in physiological conditions by fluorescence spectroscopy following the quenching of the emission of the unique fluorescent tryptophan residue within the binding site in subdomain IIA (Trp-214) (Anna, 2002).

The absorption, distribution, albumin binding and excretion of phenolic derivatives **10** in human plasma after coffee consumption have been studied, but more complex derivatives were not considered yet (Farrell et al., 2012; Nagy et al., 2011). Our data may therefore be interesting to better understand the effects of coffee consumption on the human body, as to the binding to albumin and potential competition with drugs at the same site. Moreover, we are also interested in the development of biosensing tools for the rapid detection of coffee polyphenols in quality control of coffee beverages. HSA could represent a valuable binder to be used in

such analytical devices for capturing coffee polyphenols. We have recently obtained a functional 100 aminoacid fragment of HSA, to be used as the starting scaffold to generate a library of albumin-derived binders with improved affinity and selectivity (Luisi et al., 2013).

2. Materials and methods

2.1. Materials

HSA essentially fatty acid free (A3782, ~99%), caffeic acid (⩾98%), ferulic acid (99%), 3,4-dimethoxy cinnamic acid (predominantly *trans*, 99%), chlorogenic acid hemihydrate (⩾98%) and all the reagents for the synthesis were purchased from Sigma–Aldrich Co. (St. Louis, MO, USA) and used without further purification. Polyamide MN-SC-6 0.05–0.16 mm was purchased from Macherey–Nagel (Düren, Germany).

2.2. Apparatus

Melting points were measured on a *Sanyo Gallenkamp* apparatus; the optical activity measurements ([α]) were performed with a *Perkin–Elmer 241* polarimeter at the wavelength of sodium D band (λ = 589 nm) using a quartz cuvette with a length of 10 cm (l = 1 dm); ^{1}H-NMR and ^{13}C-NMR spectra were recorded on a *Varian 500* spectrometer (scales settled on the solvents residual peaks: 7.26 ppm for $CDCl_3$ and 3.31 ppm for CD_3OD); Electrospray Ionization (ESI) mass spectrometry measurements (MS) were performed on a *Esquire 4000 (Bruker-Daltonics)* spectrometer; Infrared spectra (IR) were recorded on a *Avatar 320-IR FT-IR* (Thermo-Nicolet) spectrometer with a thin film of sample on NaCl crystal windows; Reverse Phase high-performance liquid chromatography (RP-HPLC) analyses were run on *Amersham Pharmacia Biotech* liquid chromatography equipped with *UV Amersham detector*, using a Gemini C18 3 μm 2 * 150 mm column for the analytical runs and a Gemini C18 5 μm 10 * 250 mm column for the semi-preparative ones.

2.3. Synthesis of 3,4-O-dicaffeoyl-1,5-γ-quinide (**6**)

2.3.1. 3,4-O-isopropyliden-1,5-γ-quinide (**11**)

D-(−)-Quinic acid (3.0 g, 15.6 mmol) and *p*-toluenesulfonic acid (152 mg, 0.8 mmol) were suspended in distilled acetone (150 ml). The mixture was heated under reflux (56 °C) for 48 h in a Soxhlet apparatus, which was equipped with an extraction thimble filled with molecular sieves (4 Å, Merck), activated overnight in an oven at 120 °C. The reaction mixture was cooled to 0 °C using an ice-bath; $NaHCO_3$ (364 mg, 10.3 mmol) was added and the suspension was stirred for 1 h. The mixture was filtered and the organic phase was evaporated under vacuum to obtain the product as a white solid (yield 93%). M.p. 133–136 °C; $[\alpha]_D^{25} = -30.3$ (c = 1, CH_3OH); ^{1}H NMR (500 MHz, CD_3OD): δ 1.32 (CCH_3, s, 3H), 1.49 (CCH_3, s, 3H), 2.02 (C_2-H_{eq}, dd, 1H, J_{gem} = 14.6 Hz $J_{C2Heq\text{-}C3H}$ = 3.0 Hz), 2.26 (C_6-H_{eq}, dddd, 1H, J_{gem} = 11.7 Hz $J_{C6Heq\text{-}C5H}$ = 6.1 Hz $J_{C6Heq\text{-}C2Hax}$ = 2.3 Hz $J_{C6Heq\text{-}C4H}$ = 1.4 Hz), 2.36 (C_2-H_{ax}, ddd, 1H, J_{gem} = 14.6 Hz $J_{C2Hax\text{-}C3H}$=7.7 Hz $J_{C2Hax\text{-}C6Heq}$ = 2.3 Hz), 2.53 (C_6-H_{ax}, d, 1H, J_{gem} = 11.7 Hz), 4.30 (C_4-H, ddd, 1H, $J_{C4H\text{-}C3H}$ = 6.5 Hz $J_{C4H\text{-}C5H}$ = 2.5 Hz $JC_{4H\text{-}C6Heq}$ = 1.4 Hz), 4.52 (C_3-H, ddd, 1H, $J_{C3H\text{-}C2Hax}$) = 7.7 Hz $J_{C3H\text{-}C4H}$ = 6.5 Hz $J_{C3H\text{-}C2Heq}$ = 3.0 Hz), 4.67 (C_5-H, dd, 1H, $J_{C5H\text{-}C6Heq}$ = 6.1 Hz $J_{C5H\text{-}C4H}$ = 2.5 Hz); ^{13}C NMR (125.4 MHz, CD_3OD): δ 24.54 (q, CH_3), 27.32 (q, CH_3), 35.55 (t, C_6), 38.98 (t, C_2), 72.28 (d, C_3), 72.90 (d, C_4), 73.62 (s, C_1), 76.62 (d, C_5), 110.74 (s, C_8), 180.03 (s, C_7); IR (cm^{-1}): 3583, 2932, 1777, 1315, 1161, 1075, 980; MS (ESI^+): 215 m/z (50, $[M-H]^+$), 237 m/z (100, $[M-Na]^+$).

2.3.2. 1-O-(2,2,2-trichloroethoxycarbonyl)-3,4-O-isopropyliden-1,5-γ-quinide (**12**)

Compound **11** (592 mg, 2.77 mmol) and pyridine (0.55 ml, 6.80 mmol) were dissolved in CH_2Cl_2 (6 ml). A solution of 2,2,2-trichloroethyl chloroformate (0.42 ml, 3.09 mmol) in CH_2Cl_2 (2 ml) was added dropwise to the reaction mixture at 0 °C. The solution was stirred at 0 °C for 1 h and then at room temperature for 24 h. The mixture was sequentially washed with 1 M HCl (two times, 5 ml at a time) and with brine (two times, 8 ml at a time) and the organic layer was dried on anhydrous Na_2SO_4. The solvent was eliminated under reduced pressure to obtain an orange oil. The crude was dissolved in refluxing MeOH (6 ml) and cooled, the solution was stored overnight at 4 °C to precipitate **12** as a white powder (yield 57%). M.p. 153–156 °C; $[\alpha]_D^{25} = -7.8$ (c = 1, CH_2Cl_2); ^{1}H NMR (500 MHz, $CDCl_3$): δ 1.33 (CCH_3, s, 3H), 1.52 (CCH_3, s, 3H), 2.40 (C_2-H_{eq}, dd, 1H, J_{gem} = 14.7 Hz $J_{C2eq\text{-}C3H}$ = 2.4 Hz), 2.56 (C_2-H_{ax}, ddd, 1H, J_{gem} = 14.7 Hz, $J_{C2Hax\text{-}C3H}$ = 7.7 Hz, $J_{C2Hax\text{-}C6Heq}$ = 2.3 Hz), 2.65 (C_6-H_{ax}, d, 1H, J_{gem} = 11.4 Hz,), 3.06 (C_6-H_{eq}, dddd, 1H, J_{gem} = 11.4 Hz $J_{C6Heq\text{-}C5H}$ = 6.5 Hz $J_{C6Heq\text{-}C2Hax}$ = 2.3 Hz $J_{C6Heq\text{-}C4H}$ = 1.1 Hz), 4.34 (C_4-H, ddd, 1H, $J_{C4H\text{-}C3H}$ = 5.3 Hz $J_{C4H\text{-}C5H}$ = 2.3 Hz $J_{C4H\text{-}C6Heq}$ = 1.1 Hz), 4.55 (C_3-H, ddd, 1H, $J_{C3H\text{-}C2Hax}$ = 7.7 Hz $J_{C3H\text{-}C4H}$ = 5.3 Hz $J_{C3H\text{-}C2Heq}$ = 2.4 Hz), 4.72 (C_{10}-H, d, 1H, J_{gem} = 11.8 Hz), 4.80 (C_5-H, dd, 1H, $J_{C5H\text{-}C6Heq}$ = 6.5 Hz $J_{C5H\text{-}C4H}$ = 2.3 Hz,), 4.82 (C_{10}-H d, 1H, J_{gem} = 11.8 Hz); ^{13}C NMR (125.4 MHz, $CDCl_3$): δ 24.41 (q, CH_3), 27.08 (q, CH_3), 30.34 (t, C_6), 35.42 (t, C_2), 71.15 (d, C_3), 72.46 (d, C_4), 75.47 (d, C_5), 77.09 (t, C_{10}), 78.90 (s, C_1), 94.03 (s, CCl_3), 110.21 (s, C_8), 151.50 (s, C_9), 172.61 (s, C_7); IR (cm^{-1}) 2995, 2939, 1809, 1765, 1380, 1241, 1075, 736; MS (ESI^+): 411 m/z (97, $[M^{35}Cl_3$-$-Na]^+$, 413 m/z (100, $[M^{35}Cl_2^{37}Cl-Na]^+$, 415 m/z (25, $[M^{35}Cl^{37}Cl_2-Na]^+$).

2.3.3. 1-O-(2,2,2-trichloroethoxycarbonyl)-1,5-γ-quinide (**13**)

Trichloroacetic acid (373 mg, 2.28 mmol) was added to water (42 μl) and the mixture was heated until a clear solution was obtained. When the acidic aqueous solution reached room temperature, **12** (252 mg, 0.65 mmol) was added and reaction was stirred for 4 h. Ice-cooled water (5.7 ml), ethyl acetate (11.4 ml) and 40% aqueous $NaHCO_3$ solution (11.4 ml) were added in order. The organic layer was separated from the aqueous one, that was further extracted with ethyl acetate (15 ml); the organic fractions were collected and washed with 2% $NaHCO_3$ (15 ml) and water (12 ml). The organic phase was then dried over anhydrous Na_2SO_4, filtered and the solvent was removed under vacuum to obtain a powder. The residue was crystallized from toluene to afford the product as white crystals (yield 61%). M.p. 132–133 °C; $[\alpha]_D^{25} = -4.6$ (c = 1, CH_2Cl_2); ^{1}H NMR (500 MHz, $CDCl_3$): δ 1.67 (OH, br, 1H), 2.17 (C_2-H_{ax}, dd, 1H, J_{gem} = 11.6 Hz $J_{C2Hax\text{-}C3H}$ = 11.2 Hz), 2.39 (C_2-H_{eq}, ddd, 1H, J_{gem} = 14.6 Hz $J_{C2Heq\text{-}C3H}$ = 6.7 Hz $J_{C2Heq\text{-}C6Heq}$ = 3.1 Hz), 2.68 (C_6-H_{ax}, d, 1H, J_{gem} = 11.2 Hz), 2.84 (OH, br, 1H), 3.06 (C_6-H_{eq}, ddd, 1H, J_{gem} = 11.2 Hz $J_{C6Heq\text{-}C5H}$ = 6.3 Hz $J_{C6Heq\text{-}C2Heq}$ = 3.1 Hz), 4.03 (C_3-H, ddd, 1H, $J_{C3H\text{-}C2Hax}$ = 11.2 Hz $J_{C3H\text{-}C2Heq}$ = 6.7 Hz $J_{C3H\text{-}C4H}$ = 4.5 Hz), 4.18 (C_4-H, dd, 1H, $J_{C4H\text{-}C3H}$ = 4.5 Hz $J_{C4H\text{-}C5H}$ = 4.5 Hz), 4.74 (C_9-H, d, 1H, J_{gem} = 11.8 Hz), 4.81 (C_9-H, d, 1H, J_{gem} = 11.8 Hz), 4.93 (C_5-H, dd, 1H, $J_{C5H\text{-}C6Heq}$ = 6.3 Hz $J_{C5H\text{-}C4H}$ = 4.5 Hz); ^{13}C NMR (125.4 MHz, $CDCl_3$): δ 32.65 (t, C_6), 36.53 (t, C_2), 65.86 (d, C_3), 65.95 (d, C_4), 76.20 (d, C_5), 77.11 (s, C_1), 79.04 (t, C_9), 94.03 (s, CCl_3), 151.58 (s, C_8), 171.44 (s, C_7); IR (cm^{-1}): 3412 (br), 1782, 1764, 1379, 1244, 1037, 665; MS (ESI^-): 347 m/z (20, $[M^{35}Cl_3-H]^-$), 349 m/z (20, $[M^{35}Cl_2^{37}Cl-H]^-$), 351 m/z (5, $[M^{35}Cl^{37}Cl_2-H]^-$), 383 m/z (80, $[M^{35}Cl_3-Cl]^-$), 385 m/z (100, $[M^{35}Cl_2^{37}Cl-Cl]^-$, 386 m/z (50, $[M^{35}Cl^{37}Cl_2-Cl]^-$), 389 (20, $[M^{37}Cl_3-Cl]^-$).

2.3.4. 3,4-O-dimethoxycarbonyl caffeic acid (**14**)

Caffeic acid (2.01 g, 11 mmol) was dissolved in 1 M aqueous NaOH (40 ml) and cooled to 0 °C. Methyl chloroformate (2.04 ml,

26.4 mmol) was added dropwise and the mixture was stirred for 1 h at 0 °C and for 1 h at room temperature: in a few time a yellow powder began to precipitate. The reaction mixture was acidified with 2 M aqueous HCl to pH 1, the solid was collected by filtration and washed with water. Recrystallization from 50–50 v/v water–ethanol (28 ml) gave **14** as a yellow-earth powder (yield 90%). M.p.: 140–141 °C; ^{1}H NMR (500 MHz, $CDCl_3$): δ 3.92 (OCH_3, s, 3H), 3.93 (OCH_3, s, 3H), 6.41 (C_1-H, d, 1H, J = 15.9 Hz), 7.34 (C_5-H, d, 1H, J_{ortho} = 8.4 Hz), 7.46 (C_4-H, dd, 1H, J_{ortho} = 8.4 Hz J_{meta} = 1.9 Hz), 7.49 (C_8-H, d, 1H, J_{meta} = 1.9 Hz), 7.72 (C_2-H, d, 1H, J = 15.9 Hz); ^{13}C NMR (125.4 MHz, $CDCl_3$): δ 56.10 (q, 2C, OCH_3), 118.92 (d, C_1), 122.71 (d, C_8), 123.72 (d, C_5), 127.03 (d, C_4), 133.26 (s, C_3), 142.86 (s, C_7), 144.07 (s, C_6), 144.91 (d, C_2), 153.03 (s, OCOO), 153.20 (s, OCOO), 171.58 (s, COOH); IR (cm^{-1}): 2918.7, 1760.6, 1692.6, 1632.7, 1438.2, 1265.3, 932.1; MS (ESI^-): 295 *m/z* (100, $[M-H]^-$).

2.3.5. 3,4-O-dimethoxycarbonyl caffeic acid chloride (*15*)

A suspension of **14** (1.41 g, 4.76 mmol) in thionyl chloride (2.4 ml, 33 mmol, added dropwise) was heated to 90 °C until the formation of a homogeneous brown solution without gas development (~2 h). Before stopping the reaction, the mixture was checked by ^{1}H-NMR in $CDCl_3$ to control if the chlorination was finished. The unreacted thionyl chloride was removed under vacuum and the brown solid residue was recrystallized from toluene (10 ml) and filtered to obtain **15** as a yellow powder (yield 50%), that was used immediately after its preparation. ^{1}H NMR (500 MHz, $CDCl_3$): δ 3.92 (OCH_3, s, 3H), 3.93 (OCH_3, s, 3H), 6.61 (C_1-H, d, 1H, J = 15.6 Hz), 7.38 (C_5-H, d, 1H, J_{ortho} = 8.5 Hz), 7.48 (C_4-H, dd, 1H, J_{ortho} = 8.5 Hz J_{meta} = 2.1 Hz), 7.52 (C_8-H, d, 1H, J_{meta} = 2.1 Hz), 7.76 (C_2-H, d, 1H, J = 15.6 Hz); ^{13}C NMR (125.4 MHz, $CDCl_3$): δ 56.16 (q, 2C, OCH_3), 123.36 (d, C_8), 123.89 (d, C_1), 123.97 (d, C_5), 127.74 (d, C_4), 132.05 (s, C_3), 143.01 (s, C_7), 144.96 (s, C_6), 148.21 (d, C_2), 152.81 (s, OCOO), 153.07 (s, OCOO), 165.88 (s, COCl); MS (ESI^-): 334 *m/z* (100, $[MOCH_3\text{-}Na]^+$).

2.3.6. 1-O-(2,2,2-trichloroethoxycarbonyl)-3,4-bis[3,4-O-(dimethoxycarbonyl)caffeoyl]-1,5-γ-quinide (*16*)

Compound **13** (136 mg, 0.39 mmol) was dissolved in CH_2Cl_2 (stored on $CaCl_2$, 10 ml); DMAP (10 mg, 0.08 mmol) and Et_3N (0.35 ml, 2.5 mmol) were added and the solution was cooled to 0 °C. Chloride **15** (600 mg, 1.9 mmol) was slowly added and the yellow solution was stirred for 1 h at 0 °C and then for 24 h at room temperature. The reaction mixture was sequentially washed with 1 M HCl (two times, 15 ml at a time), 2% $NaHCO_3$ (15 ml) and brine (10 ml); the organic layer was dried over Na_2SO_4 and the solvent was removed by vacuum evaporation. The crude was purified by flash chromatography on silica gel (glass column 2.5 × 35 cm, gradient elution from CH_2Cl_2/ethyl acetate 98/2 to 92/8 v/v) to obtain 16 as a pearly powder (yield 40%). ^{1}H NMR (500 MHz, $CDCl_3$): δ 2.46 (C_2-H_{ax}, dd, 1H, J_{gem} = 11.8 Hz $J_{C2Hax\text{-}C3H}$ = 11.6 Hz), 2.56 (C_2-H_{eq}, ddd, 1H, J_{gem} = 11.8 Hz $J_{C2Heq\text{-}C3H}$ = 6.8 Hz $J_{C2Heq\text{-}C6Heq}$ = 2.7 Hz), 2.71 (C_6-H_{ax}, d, 1H, J_{gem} = 11.6 Hz), 3.23 (C_6-H_{eq}, ddd, 1H, J_{gem} = 11.6 Hz $J_{C6Heq\text{-}C5H}$ = 5.9 Hz $J_{C6Heq\text{-}C2Heq}$ = 2.7 Hz), 3.89 (OCH_3, s, 3H), 3.90 (OCH_3, s, 3H), 3.92 (OCH_3, s, 3H), 3.93 (OCH_3, s, 3H), 4.75 (C_9-H, d, 1H, J_{gem} = 11.8 Hz), 4.85 (C_9-H, d, 1H, J_{gem} = 11.8 Hz), 5.02 (C_5-H, dd, 1H, $J_{C5H\text{-}C6Heq}$ = 5.9 Hz $J_{C5H\text{-}C4H}$ = 4.9 Hz), 5.36 (C_3-H, ddd, 1H, $J_{C3H\text{-}C2Hax}$ = 11.6 Hz $J_{C3H\text{-}C2Heq}$ = 6.8 Hz $J_{C3H\text{-}C4H}$ = 4.7 Hz), 5.71 (C_4-H, dd, 1H, $J_{C4H\text{-}C5H}$ = 4.9 Hz $J_{C4H\text{-}C3H}$ = 4.7 Hz), 6.28 (C_{11}-H, d, 1H, $J_{C11H\text{-}C12H}$ = 16 Hz), 6.45 ($C_{11'}$-H, d, 1H, $J_{C11'H\text{-}C12'H}$ = 15.9 Hz), 7.27 (C_{15}-H, d, 1H, J_{ortho} = 8.5 Hz), 7.34 (C_{14}-H and $C_{15'}$-H, m, 2H), 7.42 (C_{18}-H and $C_{14'}$-H, m, 2H), 7.52 ($C_{18'}$-H, d, 1H, J_{meta} = 1.9 Hz), 7.59 (C_{12}-H, d, 1H, $J_{C12H\text{-}C11H}$ = 16 Hz), 7.67 ($C_{12'}$-H, d, 1H, $J_{C12'H\text{-}C11'H}$ = 15.9 Hz); ^{13}C NMR (125.4 MHz, $CDCl_3$): δ 33.78 (t, C_2), 33.87 (t, C_6), 56.07 (q, 2C, $2OCH_3$), 56.11 (q, 2C, $2OCH_3$), 65.05 (d, C_4), 66.12 (d, C_3), 73.74 (d, C_5), 78.78 (t, C_9), 94.04 (s, CCl_3), 114.2 (s, C_1), 117.89 (d, C_{11}), 118.11 (d, $C_{11'}$), 122.45 (d, C_{18}), 122.51 (d, $C_{18'}$), 123.69 (d, C_{15}), 123.81 (d, $C_{15'}$), 127.05 (d, C_{14}), 127.23 (d, $C_{14'}$), 132.94 (s, C_{13}), 133.16 (s, $C_{13'}$), 142.83 (s, C_{17}), 142.93 (s, $C_{17'}$), 144.00 (s, C_{16}), 144.21 (s, $C_{16'}$), 144.35 (d, C_{12}), 144.94 (d, $C_{12'}$), 151.54 (s, C_8), 152.97 (s, C_{19}), 152.99 (s, $C_{19'}$), 153.15 (s, C_{20}), 153.21 (s, $C_{20'}$), 164.61 (s, C_{10}), 164.78 (s, $C_{10'}$), 170.10 (s, C_7); IR (cm^{-1}): 3583.1, 2918.0, 1771.3, 1722.2, 1441.2, 1259.7, 1146.3, 727.9; MS (ESI^+): 929.2 *m/z* (100, $[M^{37}Cl-Na]^+$).

2.3.7. 3,4-O-dicaffeoyl-1,5-γ-quinide (*6*) (Blumberg, Frank, & Hofmann, 2010)

Compound **16** (438 mg, 0.48 mmol) was suspended in dry pyridine (stored on molecular sieves, 4.4 ml); LiCl (229 mg, 5.4 mmol) was added and then the mixture was stirred for 7 days at 50 °C. During the reaction time the suspension turned to a brown solution. The solvent was removed under vacuum and the residue was dissolved in ethyl acetate (20 ml), then sequentially washed with 2 M HCl (two times, 12 ml each one), 2% $NaHCO_3$ (two times, 10 ml each one) and brine (8 ml); the organic phase was dried on Na_2SO_4 and the vacuum removal of the solvent gave an orange residue. The crude was treated by flash chromatography on polyamide MN-SC-6 (glass column 2 × 30 cm, gradient elution from ethyl acetate/methanol 80/20 to 50/50 v/v); the fractions rich in the target molecule were purified by semi-preparative RP-HPLC on a Phenomenex Gemini C18 5 μm 10 * 250 mm column (15 mg of crude for each run, loop 10 ml), using a gradient of H_2O + 0.1% TFA (A) and MeOH + 0.1% TFA (B) (20 min A 80% B 20%, from 20 to 90 min increase of B until A 40% B 60%, from 90 to 110 min A 5% B 95%, from 110 to 125 min A 95% B 5%) at a flow rate of 2 ml/min. The elution was monitored with a UV/vis detector at λ 214, 288 and 325 nm; the fractions corresponding to the peak of interest were checked with ESI^+-MS (molecular ion $[M-H]^+$ 499 *m/z*) and then freeze-dried: **6** was obtained as a white powder (yield 20%). M.p. 134–136 °C; ^{1}H NMR (500 MHz, CD_3OD): δ 2.16 (C_2-H_{ax}, dd, 1H, J_{gem} = 11.8 Hz $J_{C2Hax\text{-}C3H}$ = 11.6 Hz), 2.28 (C_2-H_{eq}, ddd, 1H, J_{gem} = 11.8 Hz $J_{C2Heq\text{-}C3H}$ = 6.8 Hz $J_{C2Heq\text{-}C6Heq}$ = 2.4 Hz), 2.47 (C_6-H_{eq}, ddd, 1H, J_{gem} = 11.9 Hz $J_{C6Heq\text{-}C5H}$ = 5.7 Hz $J_{C6Heq\text{-}C2Heq}$ = 2.4 Hz), 2.59 (C_6-H_{ax}, d, 1H, J_{gem} = 11.9 Hz), 4.92 (C_5-H, dd, 1H, $J_{C5H\text{-}C6Heq}$ = 5.7 Hz $J_{C5H\text{-}C4H}$ = 5.1 Hz), 5.18 (C_3-H, ddd, 1H, $J_{C3H\text{-}C2Hax}$ = 11.6 Hz $J_{C3H\text{-}C2Heq}$ = 6.8 Hz $J_{C3H\text{-}C4H}$ = 4.7 Hz), 5.61 (C_4-H, dd, 1H, $J_{C4H\text{-}C5H}$ = 5.1 Hz $J_{C4H\text{-}C3H}$ = 4.7 Hz), 6.14 (C_9-H, d, 1H, $J_{C9H\text{-}C10H}$ = 15.9 Hz), 6.37 ($C_{9'}$-H, d, 1H, $J_{C9'H\text{-}C10'H}$ = 15.8 Hz), 6.68 (C_{13}-H, d, 1H, J_{ortho} = 8.2 Hz), 6.80 (C_{12}-H and $C_{13'}$-H, m, 2H), 6.98 (C_{16}-H and $C_{12'}$-H, m, 2H), 7.08 ($C_{16'}$-H, d, 1H, J_{meta} = 2.0 Hz), 7.48 (C_{10}-H, d, 1H, $J_{C10H\text{-}C9H}$ = 15.9 Hz), 7.63 ($C_{10'}$-H, d, 1H, $J_{C10'H\text{-}C9'H}$ = 15.8 Hz); ^{13}C NMR (125.4 MHz, CD_3OD): δ 37.36 (t, C_2), 38.70 (t, C_6), 65.89 (d, C_4), 67.79 (d, C_3), 72.89 (s, C_1), 75.07 (d, C_5), 113.95 (d, C_9), 114.07 (d, $C_{9'}$), 114.81 (d, C_{16}), 115.34 (d, $C_{16'}$), 116.42 (d, C_{13}), 116.55 (d, $C_{13'}$), 123.41 (d, C_{12}), 123.49 (d, $C_{12'}$), 127.45 (s, C_{11}), 127.50 (s, $C_{11'}$), 146.81 (s, C_{15}), 146.89 (s, $C_{15'}$), 147.87 (d, C_{10}), 148.55 (d, $C_{10'}$), 149.81 (s, C_{14}), 150.00 (s, $C_{14'}$), 167.37 (s, C_8), 167.54 (s, $C_{8'}$), 178.22 (s, C_7); IR (cm^{-1}): 3405.7, 2950.7, 1790.6, 1633.0, 1269.35, 1020.7, 644.9; MS (ESI^+): 499 *m/z* (100, $[M-H]^+$).

2.4. Fluorescence spectroscopy

Compounds **2**, **3**, **5**, **6**, **7**, **8**, **9**, and **10** stock solutions (7 mM, 1.4 mM, 350 μM and for **6** 87.5 μM) were prepared in DMSO.

Steady state fluorescence spectra were recorded at 25 °C on a *CARY Eclipse* (Varian) spectrofluorimeter equipped with a 1 cm quartz cuvette (λ_{exc} 280 nm, λ_{em} 340 nm). The emission corresponding to λ_{exc} 280 nm was recorded in the λ_{em} range 300–400 nm. Synchronous fluorescence spectra (SFS) were measured by setting the excitation wavelength in the 240–320 nm range,

and the emission was recorded at Δ = 60 nm in the 300–380 nm range. The slit width on the excitation was set to 10 nm, on the emission to 20 nm. The concentration of HSA essentially fatty acid free solutions was 0.5 μM in 350 μl of solvent (135 μl of phosphate buffer 10 mM in Na_2HPO_4 and 2 mM in KH_2PO_4 diluted in 215 μl of mQ water, pH 7.4) for all the measurements; the ligand concentration was gradually increased during the titration from 1 μM to 500 μM by adding aliquots of their stock solutions; the final amount of DMSO was always less than 8%, and it has been verified that such amounts of the solvent do not affect the fluorescence of HSA. For compound **6** the fluorescence quenching with a titration in a narrower concentration range (from 0.25 to 200 μM) was also measured. After each addition of the ligand, the emission spectra, the fluorescence intensity, and the SFS were recorded. All the analyses were replicated three times.

The displacement of warfarin was studied with the same spectrofluorimeter and cell, in the same buffer described above for the binding study. Warfarin was added to the buffer at a 10 mM final concentration from a 1 mM reference solution in DMSO. HSA was then added at a 2.5 mM final concentration from a 250 mM reference solution in water, and the emission spectrum was recorded upon excitation of bound warfarin at 320 nM. The emission maximum was observed at 380 nM. Lactone 6 was then added at increasing concentrations by adding aliquots of its stock solution in the 400 nM–72 mM range, and the emission spectrum was recorded again at each addition.

3. Results and discussion

3.1. Synthesis of the quinide ligands

Quinide **6** has been synthesised as reported in Fig. 2, by revising and improving a methodology reported by Blumberg (Blumberg et al., 2010). Unfortunately, using the procedure reported in the literature, we always afforded a mixture of monoesters on carbons 3 or 4 of the quinide and only a small amount of the diester was achieved. It was necessary to modify it in some steps to obtain

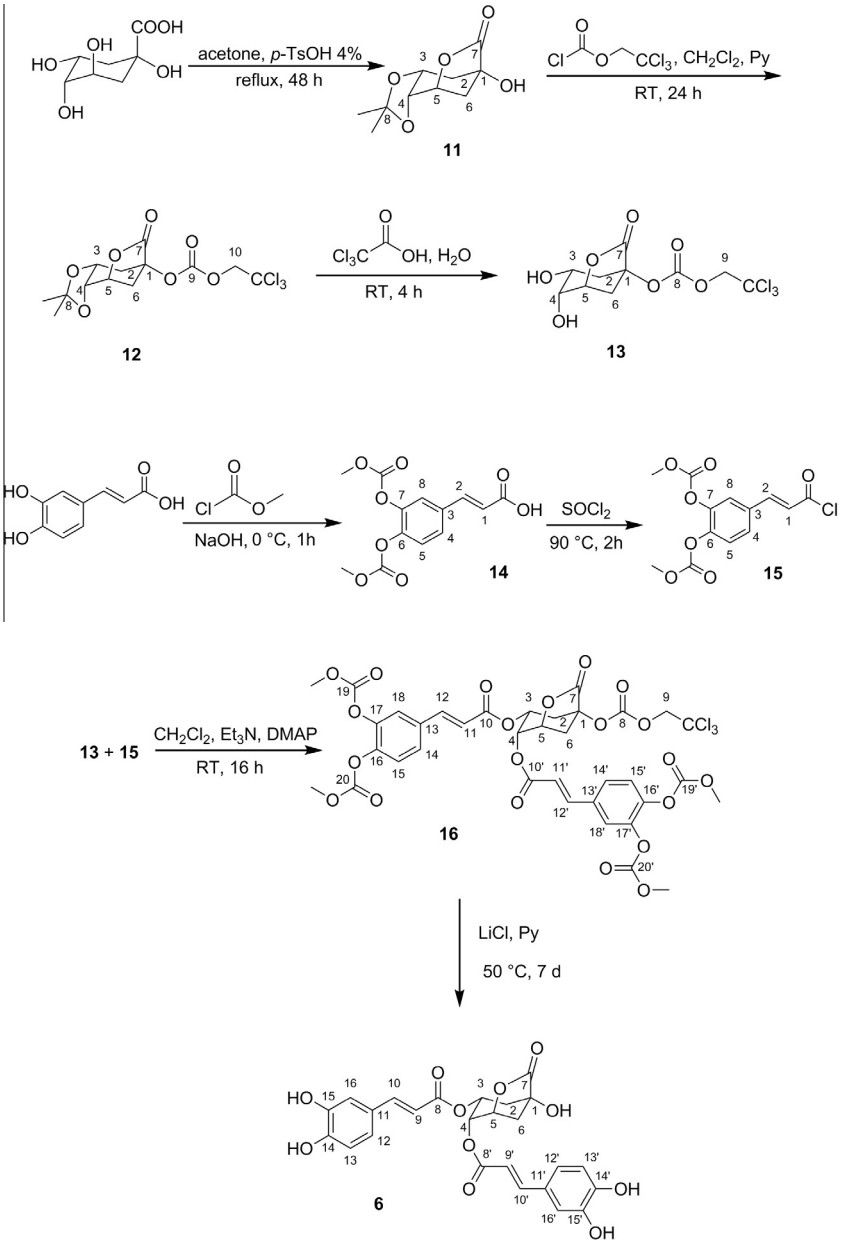

Fig. 2. Synthesis of compound **6**.

the diester as the only coupling product: we have verified that it is of the utmost importance to have the intermediates **13** and **15** in the highest purity state before carrying out their coupling, and that the maximum yield is obtained using Et_3N and DMAP as base instead of pyridine. All the intermediates were isolated as pure compounds and completely characterised by NMR spectroscopy.

The synthesis of quinides **7**, **8** and **9** have been described in details in our previous work (Sinisi et al., 2014).

3.2. HSA fluorescence and quenching

The interactions of the eight ligands with essentially fatty acid free HSA were studied monitoring the tryptophan-214 fluorescence intensity: the excitation and emission wavelengths were set to 280 and 340 nm respectively, corresponding to the excitation and emission maxima of the protein measured in the absence of ligands. Emission spectra in the range 300–400 nm were also recorded to monitor the eventual environmental changes near the fluorophore by shifts in the emission maximum wavelength, while synchronous spectra with a wavelength shift of 60 nm were also recorded to distinguish between the tryptophan and the tyrosine residues (Dockal, Carter, & Rüker, 2000). Fluorescence quenching titrations were carried out by increasing the ligand concentration while keeping the concentration of protein constant. Under these conditions only 3,4-*O*-dimethoxy cinnamic acid **10** showed interferences due to its intrinsic fluorescence emission, which is greater at lower concentrations (such self-quenching is most likely due to aggregation at higher concentrations). To avoid this interference we subtracted the blank fluorescence of this ligand from the experimental data. We have also verified that similar corrections were not necessary in all the other measurements.

HSA fluorescence quenching was observed with all the tested ligands in the same experimental conditions; in Fig. 3 the emission spectra (A) and the synchronous spectra (B) of HSA for compound **5**, taken as an example, are reported. Fig. 3A shows how the emission of the Trp residue, excited at 280 nm, changes during the titration (the fluorescence quenching full data for each ligand are reported in the Supplementary data): the emission intensity decreases while the emission maximum evidently moves to lower wavelengths and the observed blue shifts are at least of 10 nm; this shift is consistent with a change of the environmental polarity surrounding the Trp residue, resulting from replacement of the solvent in the active site by the less polar molecules of ligand (Liu, Zheng, Yang, Wang, & Wang, 2009). The use of DMSO for the ligands solutions does not contribute to the blue shift, as we have verified by adding only DMSO in the same experimental conditions of all the titrations.

A further confirmation of this microenvironmental modification near the fluorophore is given by the effects of the ligand addition on the synchronous emission spectra, as that shown in Fig. 3B, with a slight blue shift similar in all the ligands (on average the maximum shifts from 280 to 278 nm). In both the emission and synchronous spectra the fluorescence intensity decreases down to zero with increasing ligand concentration and the amount of quenching measured in the synchronous experiments replicates those obtained in the corresponding fluorescence titration, suggesting that the quenching phenomenon is related to tryptophan emission.

To determine whether the observed quenching was due to binding or collisional phenomena, the emission data were analysed according to the Stern–Volmer equation (Eq. (1)):

$$\frac{F_0}{F} = 1 + K_q\tau_0[\mathrm{Q}] = 1 + K_{SV}[\mathrm{Q}] \quad (1)$$

In Eq. (1) F_0 and F are the emission intensities before and after the addition of the quencher, respectively, K_q is the bimolecular

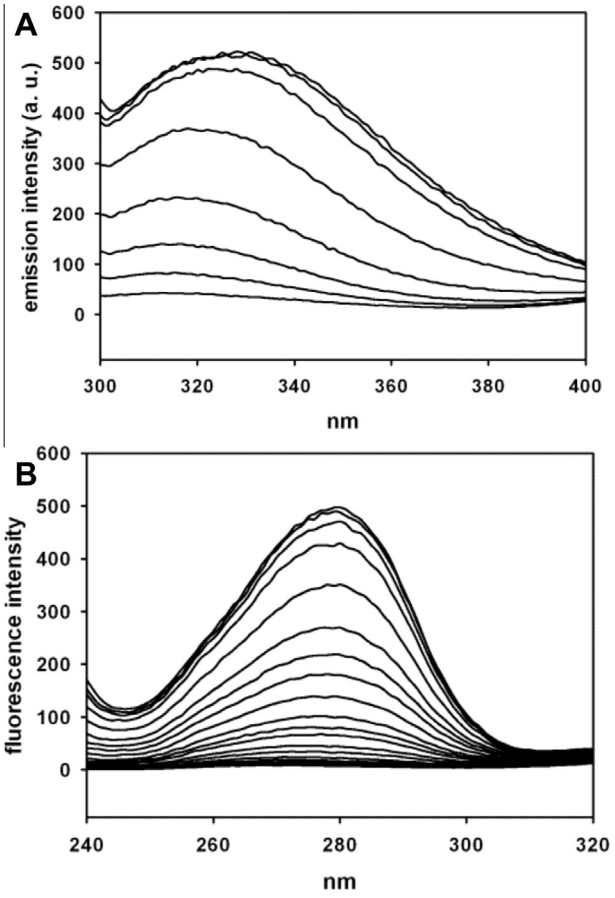

Fig. 3. (A) Emission spectra of HSA (λ_{ex} = 280 nm) in the presence of compound **5**; the concentrations of the ligands increase from top to bottom (0, 1, 5, 20, 60, 120, 180, 250 μM), while the protein concentration is fixed to 0.5 μM. (B) Synchronous spectra of HSA fluorescence emission in the presence of compound **5**; the concentrations of the ligands increase from top to bottom (0, 1, 5, 10, 20, 40, 60, 80, 100, 120, 140, 160, 180, 200, 250, 300, 350, 400, 450, 500 μM), while the protein concentration in a and b is fixed to 0.5 μM.

quenching kinetic constant, τ_0 is the lifetime of the fluorophore (for the tryptophan fluorescence decay τ_0 is about 10^{-8} s) (Kragh-Hansen, 1990), K_{SV} is the Stern–Volmer quenching constant and [*Q*] is the quencher concentration in mol/l; the protein concentration was fixed to 0.5 μM. The K_{SV} for all the ligands were determined by linear regression of a plot of F_0/F against [*Q*] (Fig. 4) in the ligand concentration range 0–140 μM, where all the plots were linear: high concentrations of molecule indeed cause a deviation from the linearity more or less evident in the different cases, probably because large amounts of ligand in solution complicate the quenching mechanism (Min et al., 2004), with the progressive increase of the dynamic quenching contribution; K_{SV} and K_q (calculated using the equivalence $K_q = K_{SV}/\tau_0$) are reported in Table 1, together with the binding parameters which will be discussed in the next section.

3.3. Dissociation constants and binding sites

The number of binding sites and the ligand–protein dissociation constants were extrapolated from the fluorescence data by a Hill analysis (Goutelle et al., 2008), using Eq. (2):

$$\log\left(\frac{Y}{1-Y}\right) = n\ \log[\mathrm{Q}] - \log\ K_D \quad (2)$$

where Y is the fraction of free binding sites (calculated as $1 - F/F_0$, assuming that the ratio F/F_0 gives the fraction of occupied binding

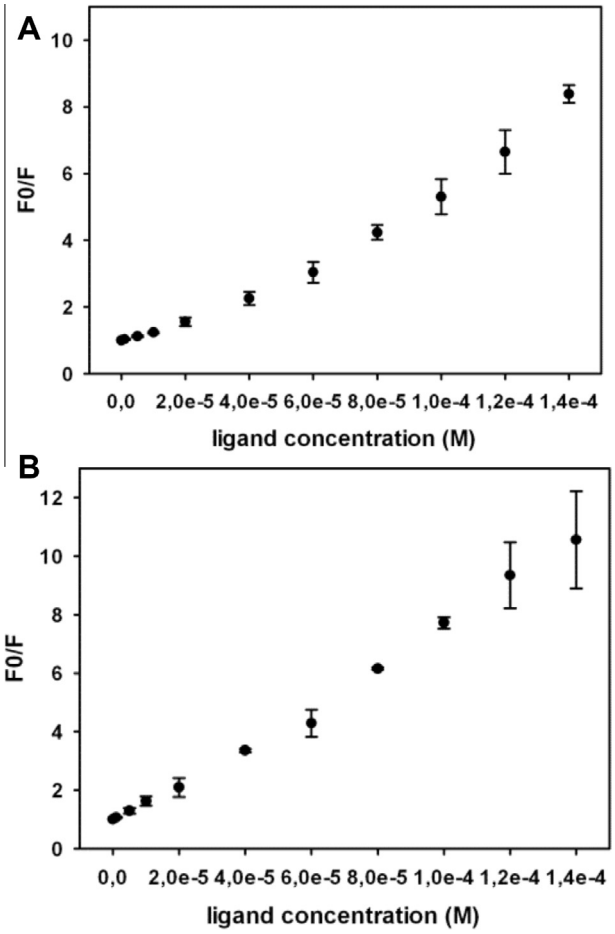

Fig. 4. Stern–Volmer plots of fluorescence quenching of HSA (λ_{ex} = 280 nm, λ_{em} = 340 nm) in the presence of compounds **3** (A), **9** (B).

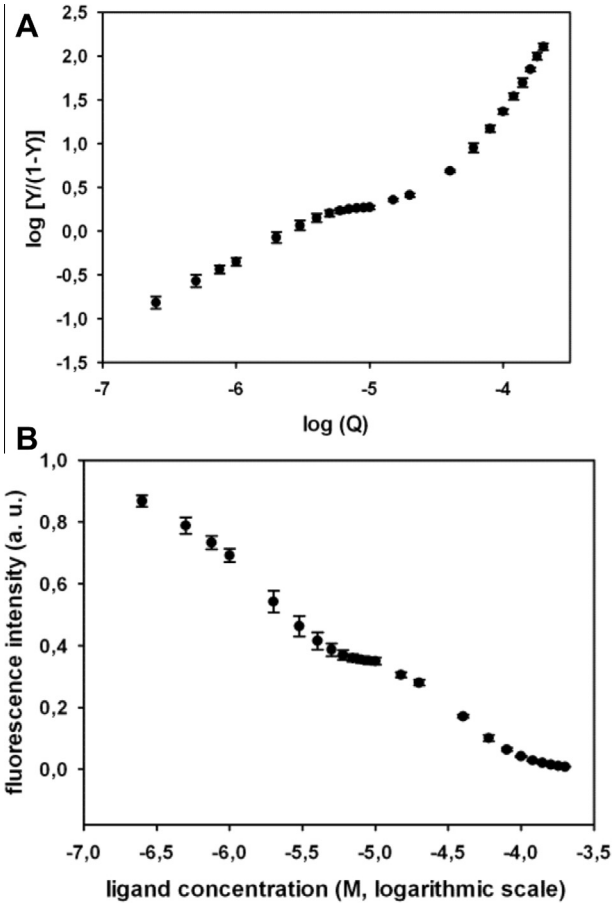

Fig. 5. Effect of the addition of compound **6** on the fluorescence intensity (the protein concentration is fixed to 0.5 μM, while the ligand concentration range is 0–200 μM) (A) and the related Hill plot (B).

sites), [Q] is the quencher concentration in mol/l, n is the number of binding sites, so it gives the stoichiometry of the interaction, and K_D is the dissociation constant.

All the ligands show linear Hill plots in the concentration range 0–140 μM, with the exception of lactone **6**. The parameters n and $-\log K_D$ for all the other ligands (Table 1) were obtained by linear regression of the Hill plot.

Compound **6** halves the fluorescence intensity even at concentrations as low as 1 μM, and to understand more about this case we decided to investigate better the interaction in the ligand concentration range 0–200 μM, keeping the protein concentration fixed to 0.5 μM. A double, consecutive sigmoidal behaviour can be clearly seen (Fig. 5A), while in the Hill plot the slope suddenly shifts from 1 to 2 (Fig. 5B). This may be due to the binding of two molecules of **6** inside the same albumin binding site. Such an unusual event in protein–ligand interaction has been recently reported for albumin, in the simultaneous binding of different drug molecules at this binding site (Yang et al., 2012).

We have evaluated the two binding constants (Table 1) by regression of the experimental data to Eq. (3) (see the Supplementary data for its derivation):

$$\frac{\Delta F}{F_0} = x\frac{\frac{[L]}{K_1}}{1+\frac{[L]}{K_1}} + (1-x)\frac{\frac{[L]^2}{K_1K_2}}{1+\frac{[L]}{K_1}+\frac{[L]^2}{K_1K_2}} \quad (3)$$

where ΔF is calculated as (F_0 – F), F_0 and F are the fluorescence intensities before and after the addition of the quencher, respectively, [L] is the quencher concentration in mol/l, K_1 is the dissociation constant for the protein–ligand complex with stoichiometry 1:1, K_2 the dissociation constant for that with stoichiometry 1:2, x

Table 1
Quenching constants according to Stern–Volmer analysis: Stern–Volmer quenching constant (K_{SV}) and bimolecular quenching kinetic constant (K_q).

	Quenching constants			Binding parameters		
Ligand	K_{SV} ± SD (10^4 L mol^{-1})	K_q ± SD (10^{12} L mol^{-1} s^{-1})	R	n ± SD	K_D ± SD (μmol L^{-1})	R
Acid **2**	8.57 ± 0.50	8.57 ± 0.50	0.98	1.20 ± 0.03	2.32 ± 0.06	0.99
Acid **3**	4.96 ± 0.26	4.96 ± 0.26	0.99	1.04 ± 0.04	21.2 ± 0.8	0.99
Acid **5**	5.29 ± 0.47	5.29 ± 0.47	0.97	1.12 ± 0.06	9.15 ± 0.48	0.99
Acid **10**	4.23 ± 0.17	4.23 ± 0.17	0.99	0.99 ± 0.03	31.1 ± 1.1	0.99
Lactone **6**	43.84 ± 4.12	43.84 ± 4.12	0.96	/	K_1 0.967 K_2 20.8	
Lactone **7**	13.75 ± 1.11	13.75 ± 1.11	0.97	1.08 ± 0.06	12.1 ± 0.8	0.96
Lactone **8**	9.81 ± 0.18	9.81 ± 0.18	0.99	1.08 ± 0.02	4.31 ± 0.06	0.99
Lactone **9**	6.86 ± 0.17	6.86 ± 0.17	0.99	1.02 ± 0.02	13.3 ± 0.2	0.99

is a coefficient that allows to take into account the different quenching efficiency in the two possible complexes.

All the tested ligands cause the HSA fluorescence quenching and both the emission and the synchronous spectra suggest that the molecules enter in the subdomain IIA and interact with Trp-214. The bimolecular quenching kinetic constants (K_q), showed in Table 1, are at least 3–4 orders of magnitude higher than the higher value for diffusion limited collisional quenching (2.0×10^{10} L mol^{-1} s^{-1}) (Eftink, 1991), thus the static quenching originating from the association of the fluorophore and quenchers in a bimolecular complex is the main contribution to the fluorescence quenching mechanism within the 0–140 μM ligand concentration range. Higher ligand concentrations complicate the quenching mechanism because the dynamic collision contribution becomes more significant.

Having thus established that the quenching data can be safely used for measuring the binding parameters, we can evaluate the results of the Hill analysis, showed in Table 1. The slope (n) in the Hill plots is near 1 for all the ligands with the exception of compound **6**, which means a 1:1 interaction stoichiometry between ligand and protein. In the case of compound **6**, the trend of the fluorescence emission intensity during the titration and the sudden slope shift from 1 to 2 in the Hill plot suggest a 1:1 stoichiometry at low ligand concentration, switching to a 1:2 ratio at higher concentrations, revealing the binding of two molecules of **6** inside the same albumin binding site, as both the molecules of **6** must be in proximity of Trp 214 in order to obtain fluorescence quenching upon binding. All the calculated K_D are in the micromolar range, showing a remarkably high affinity of these molecules for the protein. The binding constants of **2**, **3** and **5** (2.3, 21.2 and 9.2 μM respectively) are comparable in magnitude and trend to the published ones (6, 40 and 25 μM) (Hu et al., 2012; Kang et al., 2004; Min et al., 2004); among the carboxylic acids, compound **10** shows the lowest affinity, probably due to the replacement of both phenolic hydroxyl groups with methoxyl ones: this leaves only the acid moiety capable to form hydrogen bonds, that can strengthen the ligand–protein interaction (Bartolomè, Estrella, & Hernández, 2000), with the polypeptide chain within the binding site. For lactones **7**, **8** and **9**, the second has a better affinity and this may be explained as a consequence of the free hydroxyl group in position 1 on the quinide core and of the presence of two aromatic rings instead of one as in lactone **7**, enhancing the ability to establish hydrophobic interactions, and of its lower dimension compared to lactone **9**, that makes easier the entrance of the molecule in the active site.

We want to highlight the very interesting case of lactone **6**: HSA seems capable to host two molecules of it in the same binding site, and the K_1 is even in the hundred nanomolar range. To our knowledge, this is the lowest affinity ever reported for albumin, and by far more favourable than binding of most drugs to this protein. We have evaluated also the ability of lactone **6** to displace a drug from the binding site of albumin. We have chosen warfarin as this drug is the reference ligand of Sudlow site I; moreover, the intrinsic fluorescence of warfarin is strongly enhanced by the interactions with albumin, and decreases upon competition with other drugs for the protein. This phenomenon has been exploited to set up a well established method to study drug association to HSA (Sudlow, Birkett, & Wade, 1975b). The experiment was carried on a 10 μM solution of warfarin in phosphate buffer, containing 2.5 μM HSA. By adding increasing concentrations of lactone **6**, the displacement of warfarin from the albumin binding site can be clearly seen from the decrease of its fluorescence emission (Fig. 6). 50% of the initially bound drug is displaced at a 12 μM concentration of lactone **6**, while warfarin is fully squeezed out at 70 μM lactone. Data regression to a hyperbolic binding isothermal gives an apparent dissociation constant for lactone **6** of 12.4 μM at 10 μM warfarin.

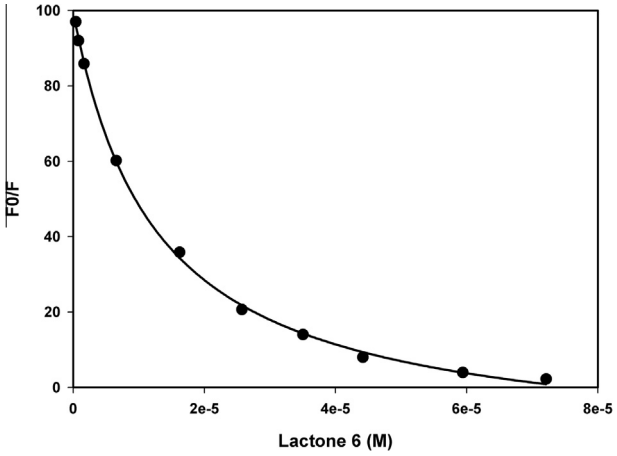

Fig. 6. Displacement of warfarin by compound **6**: the fluorescence emission of HSA-bound warfarin (excitation 320 nm/emission 380 nm) was measured on a 10 μM warfarin, 2.5 μM HSA solution. The emission decays upon addition of lactone 6 in the 400 nM–72 μM range.

4. Conclusions

In summary, we have demonstrated that HSA is able to bind all the considered ligands, with the formation of a bimolecular complex within the Sudlow site I. The dissociation constants show a very high affinity of the protein towards this family of compounds, moreover minimal changes in the chemical structure lead to significant changes in binding. A reference drug warfarin is fully displaced from albumin by low concentrations of lactone **6**: this result suggest that the dietary assumption of polyphenols from coffee and other sources could affect the pharmacokinetic profile of drugs binding to serum albumin.

Acknowledgments

We thank Dr. Filomena Guida and Professor Alessandro Tossi (Department of Life Science, University of Trieste, Italy) for the possibility to use their HPLC and for their precious help during the analysis. The University of Trieste is gratefully acknowledged for financial support.

Appendix A. Supplementary data

Supplementary data associated with this article can be found, in the online version, at http://dx.doi.org/10.1016/j.foodchem.2014.07.080.

References

Anna, S. (2002). Interaction of drugs with bovine and human serum albumin. *Journal of Molecular Structure, 614*, 227–232.

Bartolomè, B., Estrella, I., & Hernández, M. T. (2000). Interaction of low molecular weight phenolics with proteins (BSA). *Journal of Food Science, 65*, 617–621.

Blumberg, S., Frank, O., & Hofmann, T. (2010). Quantitative studies on the influence of the bean roasting parameters and hot water percolation on the concentrations of bitter compounds in coffee brew. *Journal of Agricultural and Food Chemistry, 58*, 3720–3728.

Clifford, M. N. (1985). Chlorogenic acids. In R. J. Clarke & R. Macrae (Eds.). *Coffee, Vol. 1, Chemistry* (pp. 153–202). London: Elsevier Applied Science Publ..

Clifford, M. N. (2000). Chlorogenic acids and other cinnamates: Nature, occurrence, dietary burden, absorption, and metabolism. *Journal of the Science of Food and Agriculture, 80*, 1033–1043.

Clifford, M. N., Knight, S., Surucu, B., & Kuhnert, N. (2006). Characterization by LC–MS^n of four new classes of chologenic acids in green coffee beans: Dimethoxycinnamoylquinic acids, diferuloylquinic acids, caffeoyl-dimethoxycinnamoylquinic acids, and feruloyl-dimethoxycinnamoylquinic acids. *Journal of Agricultural and Food Chemistry, 54*, 1957–1969.

de Paulis, T., Schmidt, D. E., Bruchey, A. K., Kirby, M. T., McDonald, M. P., Commers, P., et al. (2002). Dicinnamoylquinides in roasted coffee inhibit the human adenosine transporter. *European Journal of Pharmacology, 442*, 215–223.

Dockal, M., Carter, D. C., & Rüker, F. (2000). Conformational transitions of the three recombinant domains of human serum albumin depending on pH. *Journal of Biological Chemistry, 275*, 3042–3050.

Eftink, M. R. (1991). Fluorescence quenching reactions: Probing biological macromolecular structures. In T. G. Dewey (Ed.). *Biophysical and biochemical aspects of fluorescence spectroscopy* (pp. 105–133). New York: Plenum.

Farah, A., de Paulis, T., Trugo, L. C., & Martin, P. R. (2005). Effect of roasting on the formation of chlorogenic acid lactones in coffee. *Journal of Agricultural and Food Chemistry, 53*, 1505–1513.

Farah, A., Monteiro, M., Donangelo, C. M., & Lafay, S. (2008). Chlorogenic acids from green coffee extract are highly bioavailable in humans. *Journal of Nutrition, 138*, 2309–2315.

Farrell, T. L., Gomez-Juaristi, M., Poquet, L., Redeuil, K., Nagy, K., Renouf, M., et al. (2012). Absorption of dimethoxycinnamic acid derivatives in vitro and pharmacokinetic profile in human plasma following coffee consumption. *Molecular Nutrition & Food Research, 56*, 1413–1423.

Gloess, A. N., Schönbächler, B., Klopprogge, B., D'Ambrosio, L., Chatelain, K., Bongartz, A., et al. (2013). Comparison of nine common coffee extraction methods: Instrumental and sensory analysis. *European Food Research and Technology, 236*, 607–627.

Ghuman, J., Zunszain, P. A., Petipas, I., Bhattacharya, A. A., Otagiri, M., & Curry, S. (2005). Structural basis of the drug-binding specificity of human serum albumin. *Journal of Molecular Biology, 353*, 38–52.

Goutelle, S., Maurin, M., Rougier, F., Barbaut, X., Bourguignon, L., Ducher, M., et al. (2008). The Hill equation: a review of its capabilities in pharmacological modeling. *Fundamental & Clinical Pharmacology, 22*, 633–648.

He, X. M., & Carter, D. C. (1992). Atomic structure and chemistry of human serum albumin. *Nature, 358*, 209–215.

Hu, Y. J., Chen, C. H., Zhou, S., Bai, A. M., & Ou-Yang, Y. (2012). The specific binding of chlorogenic acid to human serum albumin. *Molecular Biology Reports, 39*, 2781–2787.

IUPAC Commission on the Nomenclature of Organic Chemistry (CNOC) and IUPAC-IUB Commission on Biochemical Nomenclature (CBN), (1976). *Biochemical Journal, 153*, 23–31.

Kang, J., Yuan, L., Meng-Xia, X., Song, L., Min, J., & Ying-Dian, W. (2004). Interactions of human serum albumin with chlorogenic acid and ferulic acid. *Biochimica et Biophysica Acta, 1674*, 205–214.

Kragh-Hansen, U. (1990). Structure and ligand binding properties of human serum albumin. *Danish Medical Bulletin, 37*, 57–84.

Liu, Z., Zheng, X., Yang, X., Wang, E., & Wang, J. (2009). Affinity and specificity of levamlodipine–human serum albumin interactions: Insights its carrier function. *Biophysical Journal, 96*, 3917–3925.

Luisi, I., Pavan, S., Fontanive, G., Tossi, A., Benedetti, F., Sgarra, R., et al. (2013). An albumin-derived peptide scaffold capable of binding and catalysis. *PLoS One, 8*, e56469.

Min, J., Meng-Xia, X., Dong, Z., Yuan, L., Xiao-Yu, L., & Xing, C. (2004). Spectroscopic studies on the interaction of cinnamic acid and its hydroxyl derivatives with human serum albumin. *Journal of Molecular Structure, 692*, 71–80.

Monteiro, M., Farah, A., Perrone, D., Trugo, L. C., & Donangelo, C. (2007). Chlorogenic acid compounds from coffee are differentially absorbed and metabolized in humans. *Journal of Nutrition, 137*, 2196–2201.

Nagy, K., Redeuil, K., Williamson, G., Rezzi, S., Dionisi, F., Longet, K., et al. (2011). First identification of dimethoxycinnamic acids in human plasma after coffee intake by liquid chromatography–mass spectrometry. *Journal of Chromatography A, 1218*, 491–497.

Nardini, M., Cirillo, E., Natella, F., & Scaccini, C. (2002). Absorption of phenolic acids in humans after coffee consumption. *Journal of Agricultural and Food Chemistry, 50*, 5735–5741.

Navarini, L., Colomban, S., Lonzarich, V., Rivetti, D., Brollo, G., & Suggi-Liverani, F. (2008). *Hyper Espresso Coffee Extraction: Adding Physics to Chemistry. 22nd International Studies on Coffee Science, Proceedings*, Campinas (SP, Brazil):296–309.

Olthof, M. R., Hollman, P. C. H., & Katan, M. B. (2001). Chlorogenic acid and caffeic acid are absorbed in humans. *Journal of Nutrition, 131*, 66–71.

Pal, S., & Saha, C. (2014). A review on structure-affinity relationship of dietary flavonoids with serum albumins. *Journal of Biomolecular Structure and Dynamics, 32*, 1132–1147.

Pantusa, M., Sportelli, L., & Bartucci, R. (2012). Influence of stearic acids on resveratrol–HSA interaction. *European Biophysics Journal, 41*, 969–977.

Renouf, M., Guy, P. A., Marmet, C., Fraerinf, A. L., Longet, K., Moulin, J., et al. (2010). Measurement of caffeic and ferulic acid equivalents in plasma after coffee consumption: Small intestine and colon are key sites for coffee metabolism. *Molecular Nutrition & Food Research, 54*, 760–766.

Scholz, B. M., & Maier, H. G. (1990). Isomers of quinic acid and quinide in roasted coffee. *Zeitschrift für Lebensmittel-Untersuchung und -Forschung, 190*, 132–134.

Schrader, K., Kiehne, A., Engelhardt, U. H., & Maier, H. G. (1996). Determination of chlorogenic acids with lactones in roasted coffee. *Journal of the Science of Food and Agriculture, 71*, 392–398.

Skrt, M., Benedik, E., Podlipnik, C., & Ulrih, N. P. (2012). Interactions of different polyphenols with bovine serum albumin using fluorescence quenching and molecular docking. *Food Chemistry, 135*, 2418–2424.

Sinisi, V., Boronová, K., Colomban, S., Navarini, L., Berti, F., & Forzato, C. (2014). Synthesis of mono, di and tri-3,4-dimethoxycinnamoyl-1,5-γ-quinides. *European Journal of Organic Chemistry*, 1321–1326. http://dx.doi.org/10.1002/ejoc.201301657.

Sudlow, G., Birkett, D. J., & Wade, D. N. (1975a). The characterization of two specific binding sites on the human serum albumin. *Molecular Pharmacology, 11*, 824–832.

Sudlow, G., Birkett, D. J., & Wade, D. N. (1975b). Spectroscopic techniques in the study of protein binding. A fluorescence technique for the evaluation of the albumin binding and displacement of warfarin and warfarin–alcohol. *Clinical and Experimental Pharmacology and Physiology, 2*, 129–140.

Varshney, A., Sen, P., Ahmad, E., Rehan, M., Subbaro, N., & Khan, R. H. (2010). Ligand binding strategies to human serum albumin: How can the cargo be utilized? *Chirality, 22*, 77–87.

Yang, F., Yue, J., Ma, L., Ma, Z., Li, M., Wu, X., et al. (2012). Interactive associations of drug–drug and drug–drug–drug with IIA subdomain of human serum albumin. *Molecular Pharmaceutics, 9*, 3259–3265.